Geotechnical education – Conceptual and physical models

Formation géotechnique – Modèles conceptuels et concrets

A. D.W. Sparks – *Department of Civil Engineering, University of Cape Town, Rondebosch, South Africa*

ABSTRACT : The paper describes conceptual models for visualising stress equations for partly saturated soils, models for estimating deformations from stress fields, and non-dimensional models for slope stability analysis ; plus simpler physical models such as a shear boat in which pore pressures are controlled, photoelastic models ; and simple models using elastic bands for simulating pile groups.

RESUME : Dans cette étude il s'agit d'une déscription de modèles conceptuels qui permettent d'envisager les équations de pression pour des sols partiellement saturés. Elle décrit aussi des modèles pour estimer la déformation due aux valeurs de la pression. Des modéles non spécifiques servent à analyser la stabilité du glissement du talus. Il existe aussi des modèles concrets et plus simples comme celui du "shear boat" (bateau qui glisse sur le sol) où la pression de l'eau est contrôlée ; des modèles photoélastiques ainsi que des modèles plus simples où l"emploi des élastiques simulent les pilotis.

1. CONCEPTUAL MODELS

Models are essential for educational purposes. These can be conceptual, physical or computer models. Conceptual models often require more mental concentration, and they are described first in this paper. (Physical models are suitable for junior courses. The Shear Boat is especially useful for teaching.)

2. EFFECTIVE CLAY PARTICLES

The concept of the effective particle was used in the derivation of stress equations for saturated or partly saturated soils (Sparks 1961, 1963). The effective soil particle can be defined as the solid particle plus the surrounding micelle water layer (i.e double layer). Lambe (1965, p 55) states that the thickness of the double layer is the distance from the solid particle required to neutralize the net charge on the particle, i.e. it is the distance over which there is an electrical potential.

Sridharan and others (1982) showed that particles in parallel packing move closer together when the salt concentration is increased in the pore water. It seems that the larger concentration of available cations permits the neutralization over a shorter distance, of the net charge on the solid particle. i.e. a greater salt concentration will cause thinner Micelle layers of adsorbed cations.

TABLE 1 - Brief Comparison between Parallel-packing and Edge-to-face contact of clays or silts.

FACE-to-FACE	EDGE-to-FACE contact
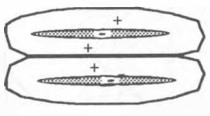	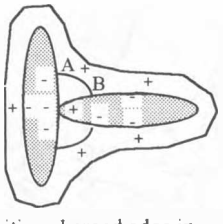
Two negatively charged solid particles are surrounded by two positively charged micelle layers. Repulsive interface between the micelle layers.	Positive charged edge in contact with negative face Attractive interface with ion chain-links AB.
Increasing salt content :-	*Increasing salt content :-*
decreases micelle thickness, decreases the repulsive force between the effective particles (if e or w constant)	provides more ions in chain-links AB, increases the interparticle contact force P_i

3. OSMOTIC PRESSURE

It was suggested that the average water pressure u'_w across the area of contact between the effective particles is greater than the value of the pressure u_w in the free capillary water . (Sparks 1961,p 4-50). The author believes that the osmotic pressure in saline water becomes evident when the salt ions are unable to move towards the unbound water because these salt ions are restrained either by a permeable membrane or because the ions are held in the adsorbed water double layer by electrical charges on the solid particles.

In other words when these water pressures are both measured by engineering pressure gauges or by levels in piezometer tubes, the water pressure in the held saline water is greater than the water pressure in the adjacent unbound water . These are the true water pressures which should be used in pressure or force equations. An "artificial" water pressure is estimated when the water pressure is calculated from vapour pressure measurements. This "artificial"water pressure is important because it is used in soil hygrometry calculations to determine the wilting tension adjacent

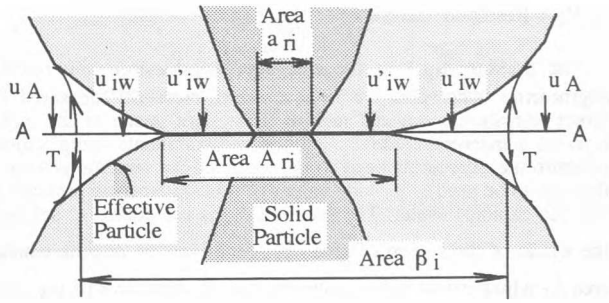

Figure 1(a) - Solid particles in contact (Sparks,1961,p4-50)

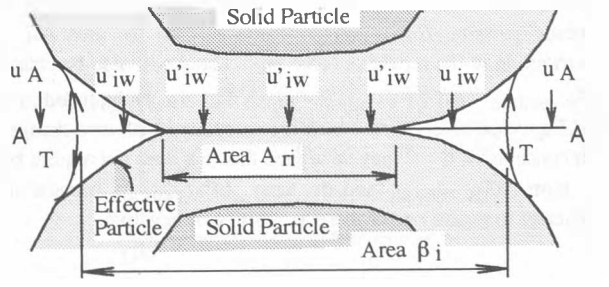

Figure 1(b) - Solid particles are not in contact

to plant roots. i.e. this "artificial" water pressure is equal to the water pressure u_w plus an osmotic pressure due to the salt concentration in the unbound water adjacent to the air-water interface. Within the micelle layer, the osmotic pressure probably increase closer to the solid particles.

It is probable that the average water pressure at the Micelle contact zone between the two effective particles is u'_w , where

$$u'_w = u_w + \Delta u_{osmotic} \qquad (1)$$

and $\Delta u_{osmotic}$ equals the osmotic pressure due to the adsorbed ions in the zone of contact between the effective particles. (i.e. on area A_{ri} in Figure 1).

Lambe also states that "since the negative charge on a clay particle is balanced by the cations in the double layer, the two advancing particles begin to repel each other when their double layers come into contact with one another." (1969, p 57).
The same concept was used (Sparks,1961, Fig 4.20) to justify a water pressure in the zone of contact between two effective particles which is different from the water pressure u_w in the free capillary water.

It has been acknowledged for many decades that clay particles can exert forces on each other even though they are not in direct physical contact. Engineers are prepared to discuss interplanetary forces which also act at a distance, and these interplanetary forces can cause an equivalent normal stress on an imaginary plane which separates two planets. This equivalent normal stress is exactly the same in concept to the "effective stress" between clay particles which are not in physical contact. The author and others such as Lambe (1969, p 244) use the term "intergranular stress" as a teaching tool to describe the "effective stress". It has been sad to note that some engineers confuse the term "intergranular stress" which can signify forces at a distance, as does "interplanetary forces", with the term " inter-grain contact stress" which refers to the stress at a point of contact between two solid particles. The latter contact stress does not need to appear in our equations.

The surface A-A between effective particles (Fig.1) can be stepped to pass through various contact zones between effective particles. Consider a portion of A-A such that the projected area of this portion of surface A-A on the horizontal plane y-z is unity.

Let :

- n = the number of contact zones between effective particles.
- P_i = the contact force between the solid grains at the i^{th} point of contact. These have zero value when the solid grains do not touch each other.
- F_{Ri} = the repulsive forces between the particles at i^{th} contact.
- F_{Ai} = the attractive forces between the particles at i^{th} contact.
- R_i = Resultant of the above 3 forces at i^{th} contact.

The pressure u_w in the free capillary water is the normal engineering water pressure (matric water pressure) measured by direct engineering devices such as a pressure gauge or the water level in a manometer tube. Indirect measurements using vapour pressure measurements need to be corrected for osmotic effects if they are to be used to provide values of this engineering pressure in the free capillary water. The pressure u_w is considered to act over the whole of the region of area β_i . But over the micelle contact area A_r which exists at the centre of area β_i there will be u_w plus an additional osmotic pressure, namely $\Delta u_{i\ osmotic}$.

The various stresses or forces can be grouped in different combinations. For example , it is convenient to consider the osmotic pressure $\Delta u_{i\ osmotic}$ which acts on the area A_{ri} as contributing to the repulsive force F_{Ri} . There will also be changes $\Delta F_{R\ osmotic}$ and $\Delta F_{A\ osmotic}$ which will also be included in F_{Ri} and F_{Ai} respectively, and which are associated with any change in salt concentration It may be argued that one does not require both the term $\Delta F_{R\ osmotic}$ and the term $\Delta F_{A\ osmotic}$ because it is sufficient to regard one of these as positive or negative.

4. THE GENERAL STRESS EQUATION

Consider the simplifying case when the air pressures are all equal to u_A , and the free capillary water pressures are all equal to u_w and consider the unit projected area of the larger surface A-A.

The following stress equation was presented publicly in 1957 (see Sparks, 1961).

$$\sigma_x = \sigma'_x + \alpha . u_A + \beta . u_w - \gamma . T \qquad (2)$$

where

- σ'_x = the normal effective stress in the x direction
  = ΣR_{xi} (summed for the n points of contact in unit area)
- α = the proportion of the unit area occupied by air.
- β = the proportion of the unit area occupied by water.
- T = the Surface tension force (approx 73 x 10^{-6} kN / m)
- γ = the length of the cut air-water boundary in the unit area.

To be more specific , the force R_{xi} consists of several forces, i.e.

$\Sigma R_{xi} = \Sigma P_{xi} + \Sigma F_{xRi} - \Sigma F_{xAi}$ (summed for n points)

where

ΣP_{xi} = x components of i^{th} inter-grain contact forces

ΣF_{xRi} = Repulsive forces
$= \Sigma F_{Ro} + \{\Sigma \Delta F_{R\ osmotic} + \Sigma (A_{ri} . \Delta u_{i\ osmotic}) \}$

ΣF_{Ro} = Repulsive forces when pore water has very low salt concentration.

ΣF_{xAi} = Attractive forces
$= \Sigma F_{Ao} + \{\Sigma \Delta F_{A\ osmotic} \}$

The values in parenthesis { } are caused by changing the salt concentration in the pore water. Because the size of the micelle layer changes when salt is added, it would be incorrect to assume that these terms in parenthesis automatically cancel each other . Sridharan and Jayadeva (1982) concluded that an increase in salt content causes clay particles in parallel packing to move closer together if the effective stress remains constant.

In summary it will be noticed that a simple stress equation (2) is found if one assumes that a change in salt concentration can be accomodated by a change in the value of ΣR_{xi} ; in other words by a change in the value of the effective stress σ'_x . If the salt concentration remains constant , then equation (2) still applies.
An increase in salt content will also increase the surface tension T.
Equation (2) also applies if the soil consists of sand or coarse silt in which the attractive and repulsive forces can be ignored. In the case of sand or silt, it follows that $\sigma'_x = \Sigma R_{xi} = \Sigma P_{xi}$.

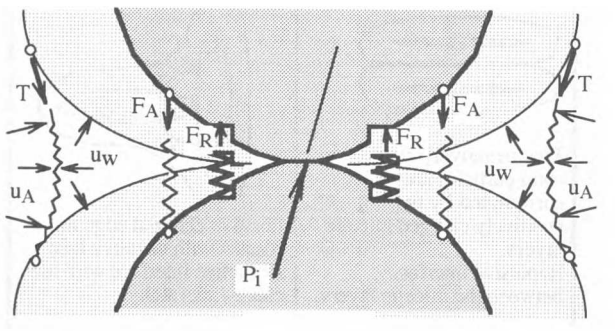

The springs represent the forces T , F_A , F_R , P_i which are shown acting on the upper particle (Sparks, 1961, p 4.83)

Figure 2 - Mechanical Model for equation (2)

5. SIMPLIFIED MECHANICAL MODEL (for Equation 2)

Springs are used to represent the forces which act between the effective particles (Fig.2). Compressive springs apply the repulsive force F_R , tension springs cause the attractive force F_A , and tension springs apply the surface tension force T. Note that the springs carrying the force T are curved due to the fact that the lateral air pressure u_A is larger than the capillary water pressure u_W . Note also that the extra water pressure $\Delta u_{i\ osmotic}$ at the contact zone between the micelle layers is also carried by the adjacent repulsive springs F_R .

6. AN APPROACH TOWARDS THE STRESS EQUATION (2)

It is convenient to regard the effective stress σ' as the unknown value in equation (2) (i.e. if the other values can be measured or estimated). Various formulae have been derived for α, β and γ in terms of the degree of saturation S_r for dense , loose and medium packings of soil particles (see Table 2, and Fig.18 and Fig.19 in the Appendix).

6.1 *For medium packing, of sands or silts :-*

It is suggested that the formulae in Table 2 can be used over the whole range of the degree of saturation S_r. The value of S_r in these formulae is a ratio between zero and unity. It is suggested that the value of 'r' for sands and silts is equal to $r = 0.5 \times D_{15}$.

TABLE 2 - Suggested formulae - Sands / silts - Medium Packing

$$\beta = 0{,}7\,(S_r)^{0,5} + 0{,}3\,(S_r)^{6}$$

$$\alpha = 1 - \beta$$

$$\gamma . r = 2{,}2\,(S_r)^{0,25}\,(1 - S_r)^{0,25}$$

$$(u_A - u_W) = 6.\,T \,/\, \{\,(S_r)^{0,9} . r\,\}$$

where $T = 73 \times 10^{-6}$ kN / m

See Appendix for curves of β and γ .

Using these formulae for sands and silts leads to non-dimensional general solutions for u_W as shown in Figure 3. The grain size is introduced via the parameter r (i.e.radius of effective soil particle).

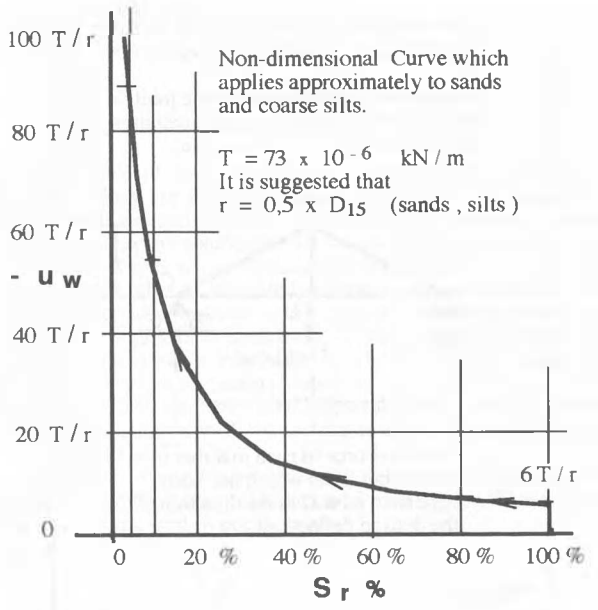

Figure 3 - Non-dimensional Drying Curve

7. SLOPE STABILITY

Various simplified methods have been developed for circular and non-circular slides. These include methods to calculate the risk of failure (Sparks,1996). However it is also useful to calculate bearing capacity factors for foundations by using slope stability techniques . These tend to underestimate the bearing capacity factors. Non-dimensional parameters are used wherever possible.

7.1 *Numerator for the Factor of Safety*

Students are urged to only place the strength terms involving cohesion c and tan Φ (and reinforcement strength if it exists) in the numerator of the expression for the Factor of Safety. This is irrespective of the method of analysis. All other terms are in the denominator. The Factor of Safety is then equal to the Factor of Safety with respect to Strength. The equation (3) is an example. It applies to the slope in Figure 4.

$$F_S = \frac{c.\,\Sigma\,(\Delta L) \;+\; \mathrm{Tan}\,\Phi .\,(\Sigma\ P_n)}{\Sigma\,(W.\,\mathrm{Sin}\,\alpha) + \{\,\Sigma\,(y.\,W_{horiz}) - z.\,P_W\,\} / R} \qquad (3)$$

If F_S is constant, it can be shown that a linear relationship exists between the non-dimensional variable $c / (\gamma .\ H_W)$ and Tan Φ ; where " H_W " is a characteristic working height, such as the total slope height (Sparks, 1965).

For each trial failure surface a straight line (for F_S = constant) can be plotted either on the " c versus Tan Φ " diagram or on the "$c / (\gamma .\ H_W)$ versus Tan Φ " diagram. Failure combinations of $c / (\gamma .\ H_W)$ and Tan Φ lie on an envelope to these straight lines as in Figure 5. With reference to Figure 5, the point X represents the measured values of cohesion c and Tan Φ .

The Factor of Safety with respect to Shear Strength is

$$F_S = (\text{Distance OX} \,/\, \text{Distance OA}) \qquad (4)$$

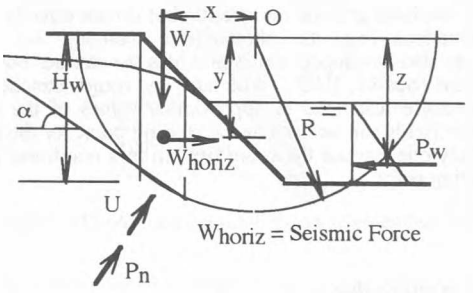

Figure 4 - Simplified System

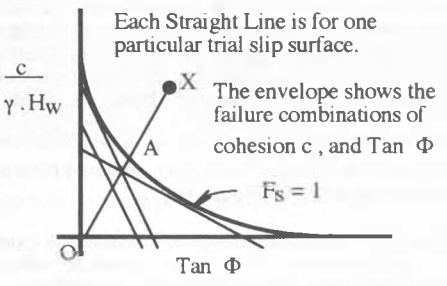

Figure 5 (Sparks , 1965)

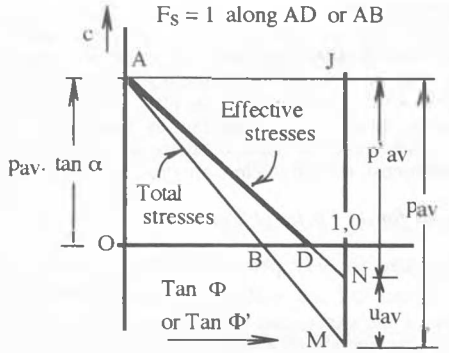

Figure 6 - A simpler method for Stability Analysis

7.2 *Simplified quick estimates for Slope Stability* :-

A method was published (Sparks,1975) which allows a quick estimate of the combinations of c and Tan Φ which correspond to a Factor of Safety equal to unity i.e. this provides the straight line on the "c versus Tan Φ " diagram for a particular trial slip surface.

One can consider either the usual effective stress analysis or the total stress analysis (e.g. for quick construction). In Figure 6, p_{av} , p'_{av} and u_{av} are respectively the average total pressure, average effective pressure and the average pore pressure normal to the trial slip surface. The angle α is a weighted average of the slope α of the slip surface (weighted according to total weights of slices).
The order of construction is to plot points O, A, J, M, and N.
The required strength lines for F_S = 1 are AD or AB.

8. PROPOSED MODEL - ESTIMATION OF DEFLECTIONS

An engineer might wish to check the order of magnitude of the deformation of a certain point in a continuum. The author derived the following method as a quick method, but it can also be used for serious accurate estimates. The method applies to two dimensional or three-dimensional systems, but this same method also applies to linear or non-linear strains. This method provides deformations.

Certain methods provide the stresses but do not directly provide the deformations (e.g. the photo-elastic method). An iterative method was also developed which provides the stresses but not the deformations (Sparks, 1983). Alternatively, rough sketches of the stress trajectories can lead to approximate values of the stresses. These stress fields can be used as the starting point for the method. Alternatively one can use the strain field from a non-linear analysis as the starting point.

8.1 *Steps in this method* :-

A problem with a known solution has been chosen, so that this solution can act as a check on the method (i.e. a deep beam, which is a plane stress problem. See Figure 7a).

a.) The two-dimensional or three-dimensional stress field is loaded with the required stress field. Two identical pinjointed structures will be considered. One of these will be superimposed on the stressed continuum. This stressed structure will be considered to be the "real structure" whose members are being stretched or compressed by the stress field. (see Fig. 7b). This real structure can consist of several members chosen to avoid unstressed holes or voids in the continuum.

b.) It is required to find the deflection (in a certain direction) of the point D relative to the point A (Figure 7a).

c.) Use the known continuum stresses to estimate the extension or shortening of the members of the "real structure" described in step (a) . These have been written in the second column of Table 3 (with algebraic signs, e.g. extension positive).

The Real Stress Field
and the "real structure"

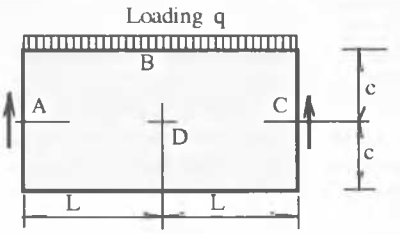

Deep Beam supported at A and C
Consider the case when c = L = 2 m
Thickness = 0.1 m. q= 10 kN / m
Poisson's ratio = 0.3

Fig. 7 (a)

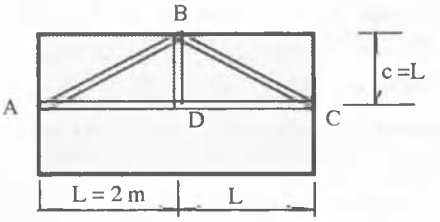

In one's imagination cut the stressed structure ABCDA out of the Stress Field. Estimate the extension or shortening of each member AB,BC, CD, DA and BD. (See equation 5 for quick methods for estimating these.)

Fig. 7 (b)

Chosen Complementary Structure
to carry the unit load at point D

It is required to find the vertical deflection at D relative to the centre-line points A and C.

Choose a pin-jointed structure which is supported at A and C as shown (use rollers where needed).
The structure is anchored at A,because it is desired to find the deformation of point D relative to the point A.

Apply a unit vertical loiad to the joint D in the direction in which one requires the deflection of D in Figure 7(a).

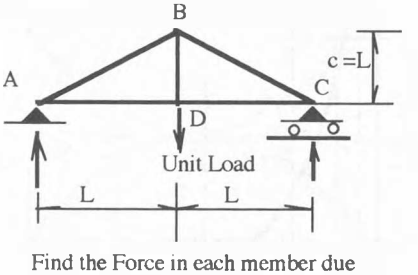

Find the Force in each member due to the Unit Load which has been applied at joint D in the direction of the desired deflection.

Fig. 7 (c)

Table 3 - Summary of proposed simple method for estimating Deflections in Stress Fields (refer to example in Figure 7 a)

Member	Extension (+) or Shortening (-) in Figure 7b. Average Strain x Member Length	Multiplier.(+ or -) i.e. Force due to unit load at D in Fig 7c.	Extension (+ or -) x Multiplier (+ or -) x Number of members
AD and DC	(- 15 / E) x 2 m	+ 1	(- 30 / E) x 2 No = - 60 / E
AB and BC	(- 156.8 / E) x 2.236 m	- 1.118	(+ 392 / E) x 2 No = + 784 / E
BD	(+ 63.1 / E) x 1 m	+ 1	= + 63.1 / E
Settlement of point D relative to the centre points A and C (in Figure 7a) = algebraic sum = 787 / E			
Check :- Lengthy formula (Timoshenko & Goodier , equation 34, page 43) provides settlement of point D = 785 / E Answer from above method is within 0.25 per cent.			

d.) The second pin-jointed structure (Fig 7c) has the correct support conditions (point A anchored) and a similar geometry to the "real structure" chosen in step (1). Apply a unit load to the joint D in the direction of the required deflection component. Find the forces (with algebraic signs; tension positive) in each of the members of this second pin-jointed structure. These forces are the multipliers used in the last portion of equation 5. (See Table 3).

e.) Now estimate the required deflection of point D in the direction of the unit load, by using the following formula :-

$$\text{Deflection of D relative to A} = \Sigma \ (\Delta 1_i \cdot F2_i) \qquad (5)$$

where Σ = Summation for all members.

$\Delta 1_i$ = Extension of member i in the "real structure"

and $F2_i$ = Force (i.e. multiplier) due to unit load in the second structure.

For two-dimensional stresses (plane stress) :-

$\Delta 1_i$ = Length member . ($\sigma_t - \nu . \sigma_n$) / E

σ_t = Average continuum stress in direction of member

σ_n = Average continuum stress normal to member

ν = Poisson's ratio

E = Young's Modulus

For three-dimensional stresses :-

$\Delta 1_i$ = Length member . ($\sigma_t - \nu . \sigma_{n1} - \nu . \sigma_{n2}$) / E

For non-linear analysis :-

$\Delta 1_i$ = Average Strain x Member Length

9. CERTAIN PHYSICAL MODELS

Only a selection of the physical models used by the author will be described. Many are simple and require little effort to assemble. These models can stimulate the interest of students in more formal methods, and are not a substitute for formal teaching methods.

A model which is not described in this paper is a model of interconnected tubes to simulate isochrones for consolidation. The model is inverted in order to start its process. The student can also calculate the degree of consolidation by measuring the volume of outflow water. Another spectacular model uses Moiré fringes to show bulbs of pressure under foundations.

A model which required more preparation was a model which simulated the settlement of Venice due to the pumping of ground water (Sparks, 1977, Fig.7).

Devices were made which easily measured the thrust, the shears, and the moments at the heads of model piles. These were shown at a piling conference in London.

10. PHOTOELASTIC MODELS

One of the most instructive models is that of a point load P adjacent to a soil trench (See Fig 8). As the load is applied, the student will see the growth of a concentrated band of shear stresses on the critical plane between the point load and the base of the cut.

11. SEEPAGE TANKS

Large and small seepage tanks have been constructed in which the author constructed piezometer tubes within the perspex walls of the tanks.(See Fig 9). Such tanks must be at least 100 mm wide to allow hand entry. "Null-flow" quick response piezometer tubes were designed to measure dynamic pressures. Photography was used to record piezometer levels. Later, electronic transducers were coupled to computers to measure dynamic water pressures in small seepage models. Portable tanks using the Hele-Shaw viscous flow analog have been constructed for use on overhead projectors. These illustrate free-surface seepage patterns.

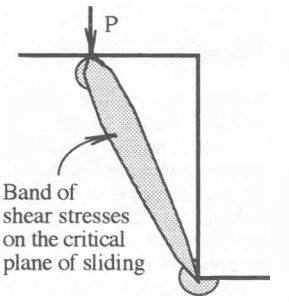

Figure 8 - Photoelastic model shows stresses due to Force P

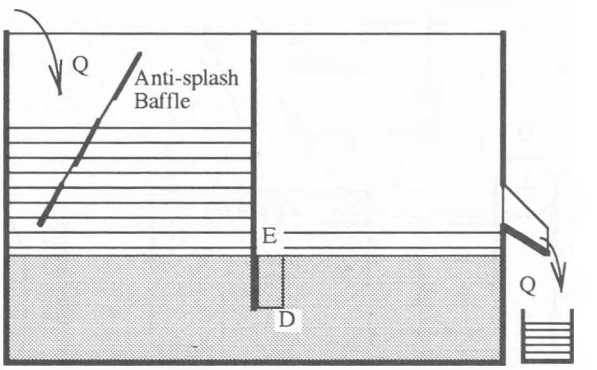

Figure 9 - Seepage Tank to illustrate toe heave at E.

12. SHEAR BOAT AND ITS USES

The shear boat has been used as a most useful teaching aid. (See Fig 10). It is used to teach several principles. It is probably the simplest shear box in which sand can be tested at different water pressures. The shear boat is a rectangular box which was constructed from perspex (1965) . The base of the box has a slight upward curve (like a sledge) at T, and the underside is serrated along its entire surface with deep sharp grooves which key into the levelled sand.

The total weight W of the shear boat can be varied via internal weights K. The bouyant uplift force U is equal to the total weight of displaced volume of water, and U can be varied by adjusting the height of water h. The dividing wall V is slotted down to the top of the sand, so that a thin stainless steel cable can pass from T on the shear boat, and around the pulleys R and Q to the rectangular tin into which water is slowly poured to cause the shear force F required to move the boat. To achieve partly saturated conditions, the levelled sand is first submerged, the shear boat is placed in position, and then drainage occurs via porous sintered glass discs into the lowered water well J, where the water level is kept at the desired level. The degree of saturation of the sand can be calculated from the volume of water which flows out of the system.

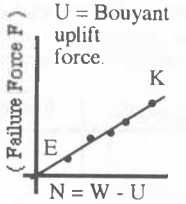

Figure 11 (a)

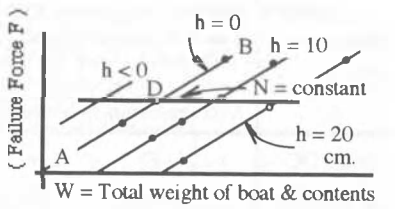

Figure 11 (b)

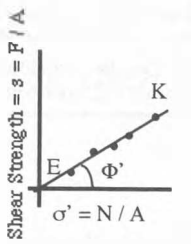

Figure 11 (c)

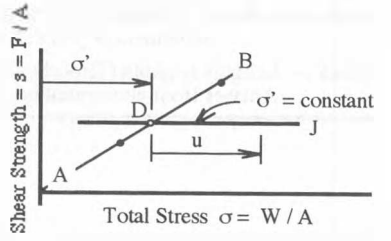

Figure 11 (d)

12.1 *This device can be used to investigate the following :-*

a.) The shear strength of dry, saturated or partly-saturated sands,
b.) The effect of pore pressures on the shear strength of sands,
c.) The dilation effects of sand during shear (if required).
d.) The $\Phi = 0$ Mohr strength envelope for certain conditions.
e.) Visualization of the shear strength envelopes for clay from discussions of the shear strength envelopes for sands.
f.) According to Bishop and Skempton the Chi Factor χ for partly saturated soils lies between zero and unity. The author showed that this factor can be very large (Sparks 1963).

This apparatus proved beyond any doubt that the Chi Factor χ can be greater than unity. And this same result was achieved by a different apparatus (Sparks, 1963, Vol 2, p 90).

g.) However its greatest strength as a teaching aid can be illustrated by the measured curves shown in Fig 11 .

12.2 *One method for use of this apparatus :-*

a.) First the sand is tested dry. Failure combinations of F and W yield the curve AB in Figure 11 (b).
b.) Water is now introduced so that h = 10 cm. The total weight W must be increased to prevent flotation. New failure values of F and W yield a different curve in Fig 11 (b).
c.) Step 2 is repeated with h = 20 cm, to yield a new curve.
d.) The students are asked to calculate the net force N=W-U from each of the previous readings, and to plot the results as in Figure 11(a). The points all lie on the same line EK. This illustrates that the effective force N controls F values.

(i.e. Shear strength depends upon the effective stress σ').

e.) The student is asked to choose any point D on the curve AB (Fig 11b). Because u=0 on AB, the value of N is equal to W. Now seek a point on the curve h=10 cm (Fig 11 b) which has the same value of N. i.e. we can calculate U for h=10 cm and add this to the N value from curve AB, to find the W value on the curve h=10 cm. Similarly find points with the same N value on the curve h=20 cm . Draw a line through D which best fits the points for which N is constant. The line will probably be horizontal.
f.) Divide each of the variables F , N and W by the plan area A of the shear boat to convert the curves in Figs 11(a) and 11(b) to the stress curves for sand in Figs 11 (c) and 11(d).
g.) Certain concepts for clays can be introduced via the sand tests. If several saturated clay samples were to be sheared at the same water content (i.e. undrained) we would expect the same shear strength (i.e. line DJ in Fig 11d) , but points on this line all coincide with one point on the curve EK in Figure 11(c). The points on EK could each be obtained by starting with a soft mixture at state E, allowing drainage under the effective stress σ' (which will increase the clay strength), and then slowly testing the clay to give a point on EK.

13. TILTING SLOPE MODELS

Various tilting devices were constructed to test model slopes. Sand was placed in the apparatus and deep-seated slip surfaces were arranged by using suitable baffles. It was interesting to note that in most cases the Bishop theory predicted the failure even though use was made of sand which was being tested in an unatural system (i.e. deep-seated failures).

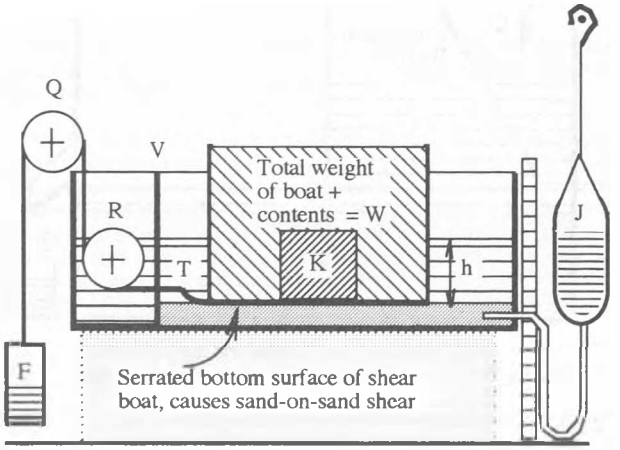

Figure 10 - Shear Boat (1965)

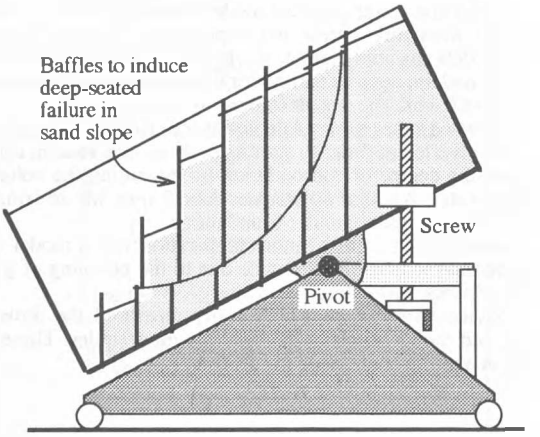

Figure 12 - Movable Tilting Apparatus.

14. MODELS USING ELASTIC BANDS

14.1 *Simulation of the "void ratio - log pressure" curve*

The apparatus in Fig.13 was constructed (1965) to simulate a "void ratio versus log effective pressure" curve. This model is simple for students, but the lecturer must emphasise that in the case of real soils one must determine this curve by testing the real soil in the laboratory oedometer or triaxial K_o test.

The distance AC can be 10 cm, and the initial position of the knot B_o is midway between A and C. The force P in the rubber band BN can be estimated by measuring the extension of this rubber band. The distance Δ is proportional to the void ratio e. Scaling factors are used to find σ' from the force P, and the void ratio e from the distance Δ .

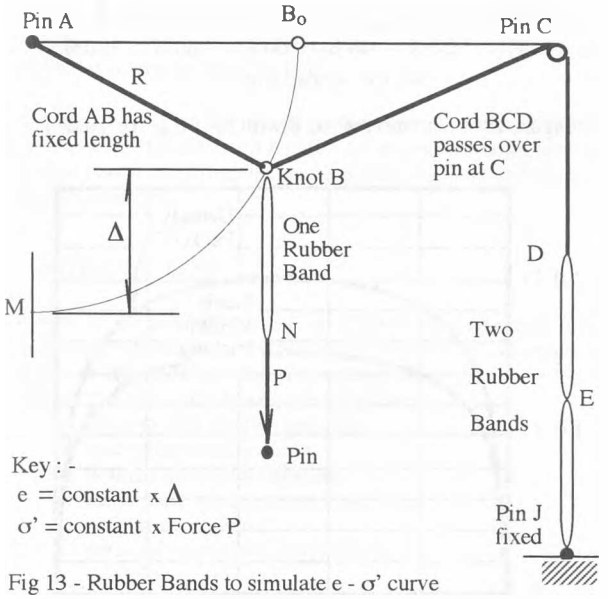

Fig 13 - Rubber Bands to simulate e - σ' curve

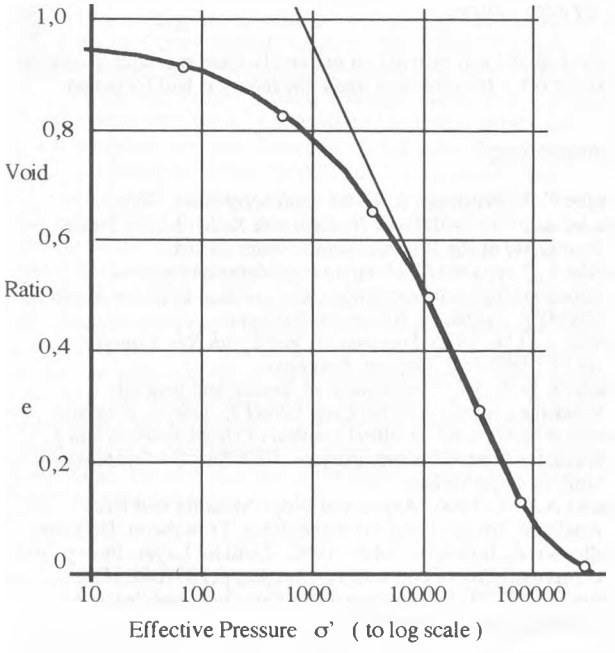

Fig. 14 - Typical curve simulated by elastic bands

14.2 *Rubber bands for two-dimensional pile systems*

Rubber bands were used to simulate piles in pile systems (1965). The model can be used within a small frame on an overhead projector, followed by hands-on experimentation by students. The main objective is to decide which piles are in tension, and how to find a more suitable pile layout. The forces in the piles can also be estimated from the extensions of the rubber bands.

Consider the pile system shown in Fig. 15(a). The force JK is the resultant applied load from the soil and from hausers of ships. A piece of cardboard is cut to the shape of the pile cap. Students should then be asked to comment on the validity of the two different models shown in Fig 15(b) and Fig 15(c). When using the models a correct solution will exist only if the rubber bands are parallel to the piles, and if the pile cap is not tilted.

Students are asked to investigate the criteria which might cause a pile to be in tension. They will learn that if the pile AB is ignored, the applied force JK must act through the intersection of the lines of action of piles AC and DE. It will also be found that in order to prevent the pile cap from tilting, and in order to have the correct lines of action for the rubber bands, it may be necessary to swop over the achorage point for the rubber band for a tension pile such as AB (as shown by the solid arrows in Fig 15(b) and Fig 15(c).)

14.3 *Forces in three dimensional pile groups*

This apparatus constructed in 1965 is easy to use. (See Fig. 16) Peg-board (which contains many holes) was used for the horizontal surfaces and for the moveable pile cap. Similar elastic pieces were used for the pile forces. Pipe cleaners were attached to one end of each elastic band; while the other end of each pipe cleaner was bent into a loop through which the far end of the elastic band could slide. The fur could be burnt off each loop in order to expose the wire of the pipe cleaner. The extensions of the elastic bands were measured from these loops, and hence the relative forces in the piles could be estimated. Horizontal, vertical forces and even couples (about horizontal or vertical axes) can be applied to the pile cap. The elastic bands are attached to thin

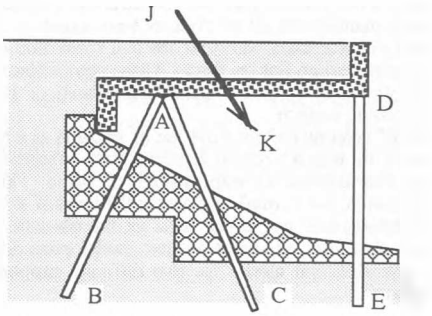

Figure 15 (a) - Typical Harbour Quay

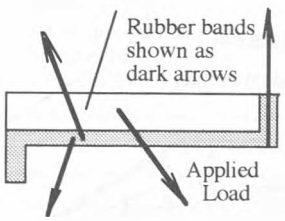

Figure 15 (b) - Force directions maintained

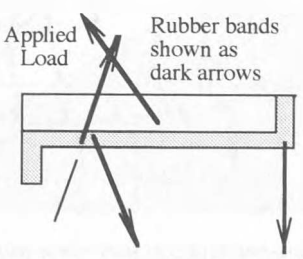

Figure 15 (c) - Force directions inverted

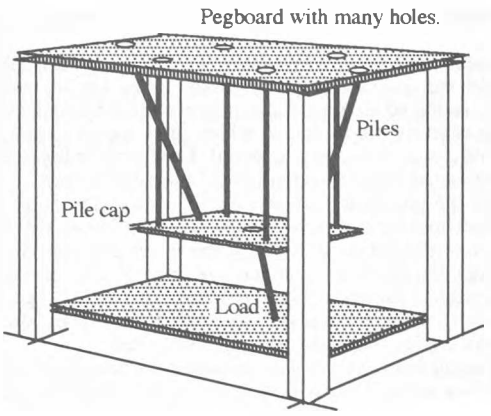

Figure 16 - Elastic bands used for 3-dimensional pile group. Pile system inverted, and all forces are tensile. Elastic is tied to strings anchored on boards.

strings, and the anchorage ends of the thin strings are fixed and re-adjusted on the peg boards until a correct solution is obtained.

The correct solution is obtained when the lines of action of the elastic bands co-incide with those of the proposed piles, and when the pile cap remains stationary. An advantage of this model is that it will also show how the pile cap is likely to twist (e.g. about the vertical axis, or a horizontal axis.). The solution from this simple model is obviously a solution which neglects the lateral restraining forces which act on the piles from the soil. If necessary weaker elastic bands can be used in the horizontal plane to simulate these forces.

15. GELATINE TO RECORD FAILURE SURFACES

Vertical bands of coal dust were placed between white sand prior to bearing capacity failure on a slope (1962) (see Fig.17). An impermeable sheet (e.g. plastic) had been placed in the soil around the zone of interest.

After failure, a hot gelatine mixture was carefully poured into the sand in such a manner that all air pockets were expelled. An anti-bacteria chemical was used. Slices of the soil were then carefully cut out and supported on flat tin sheets. These were allowed to dry in the shade and they formed a permanent record of the three-dimensional failure surface.

Other uses of gelatine included the use of gelatine as a binder in a coarse sand in which erosion patterns were observed when warm water was allowed to seep through the sand. These tests proved that erosion due to outflow starts at the level of an external free water surface, and not at the level of the phreatic surface. Gelatine was also allowed to set around model piles. The piles buckled in two different modes for two different proportions of gelatine mixture.

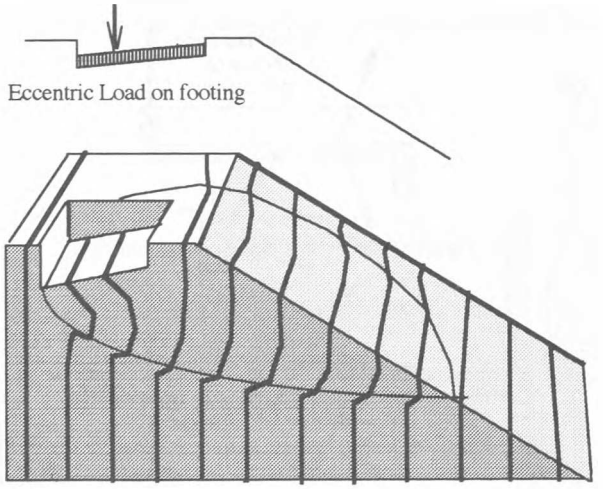

Figure 17 - Vertical bands of coal show shear pattern on centre line

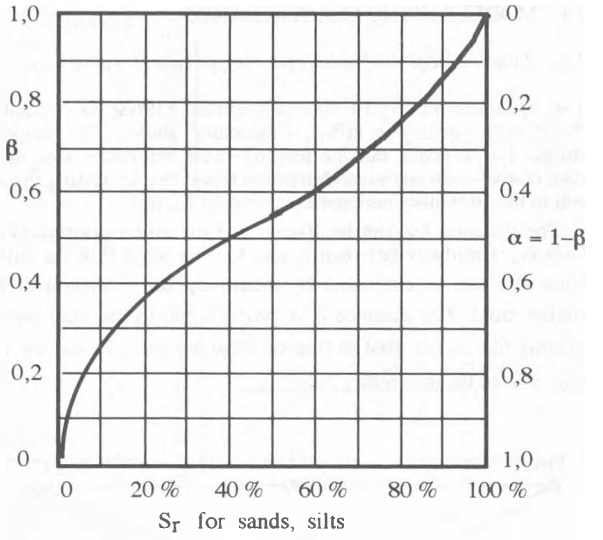

Figure 18 - Variation of α, β with S_r (e.g. for sands.)

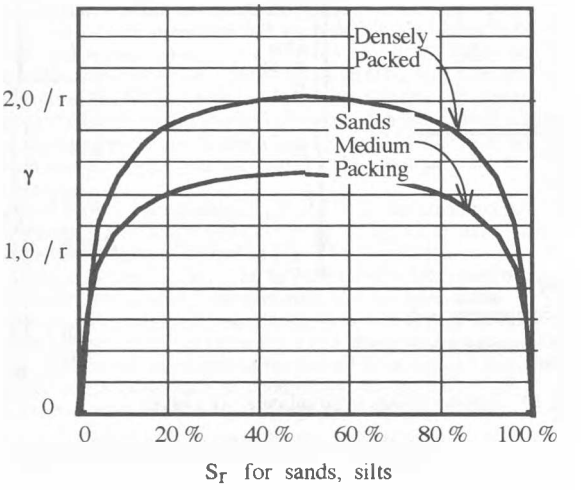

Figure 19 - Variation of γ with S_r (e.g. for sands).

16 CONCLUSION

A good model can provide an extremely clear message. A simple model is often remembered when the theory is half forgotten.

REFERENCES

Lambe T.W.,Whitman R.V.1969.*Soil Mechanics*, Wiley,

Sparks A.D.W. 1961.*Partially Saturated Soils*, M.Sc. Thesis, University of the Witwatersrand, South Africa.

Sparks A.D.W. 1963.Theoretical considerations of stress equations for partly saturated soils, *3rd Reg Conf for Africa* , ISSMFE, Salisbury, Rhodesia, Balkema.

Sparks A.D.W. 1975. Discussion, Vol 2, *6th Reg Conf for Africa* , ISSMFE, Durban, Balkema.

Sparks A.D.W. 1977. Settlement of Venice and general estuarine deposits, *9th Int Conf ISSMFE*, Tokyo, Balkema.

Sparks A.D.W. 1983. A direct method of stress analysis and a check for Finite Element analyses, *FEMSA / 83 Symposium*, Univ of Cape Town.

Sparks A.D.W. 1996. Aspects of Slope Stability and Risk Analysis, *7th Int.Symp. on Landslides*, Trondheim, Balkema.

Sridharan A.,Jayadeva; M.S. 1982. Double Layer theory and compressibility of clays, *Geotechnique*, p 133-144, ICE.

White R.E. 1979. *Introduction to the Principles and Practice of Soil Science*, Blackwell.

APPENDIX - Curves for equation 2 and Table 2